Supplement of Hydrol. Earth Syst. Sci., 26, 2113–2129, 2022
https://doi.org/10.5194/hess-26-2113-2022-supplement

Hydrology and Earth System Sciences
Open Access
EGU

Supplement of

Stochastic daily rainfall generation on tropical islands with complex topography

Lionel Benoit et al.

Correspondence to: Lionel Benoit (lionel.benoit@inrae.fr)

1 Supplementary material 1: Bivariate scatterplots of latent values in the island of O‘ahu

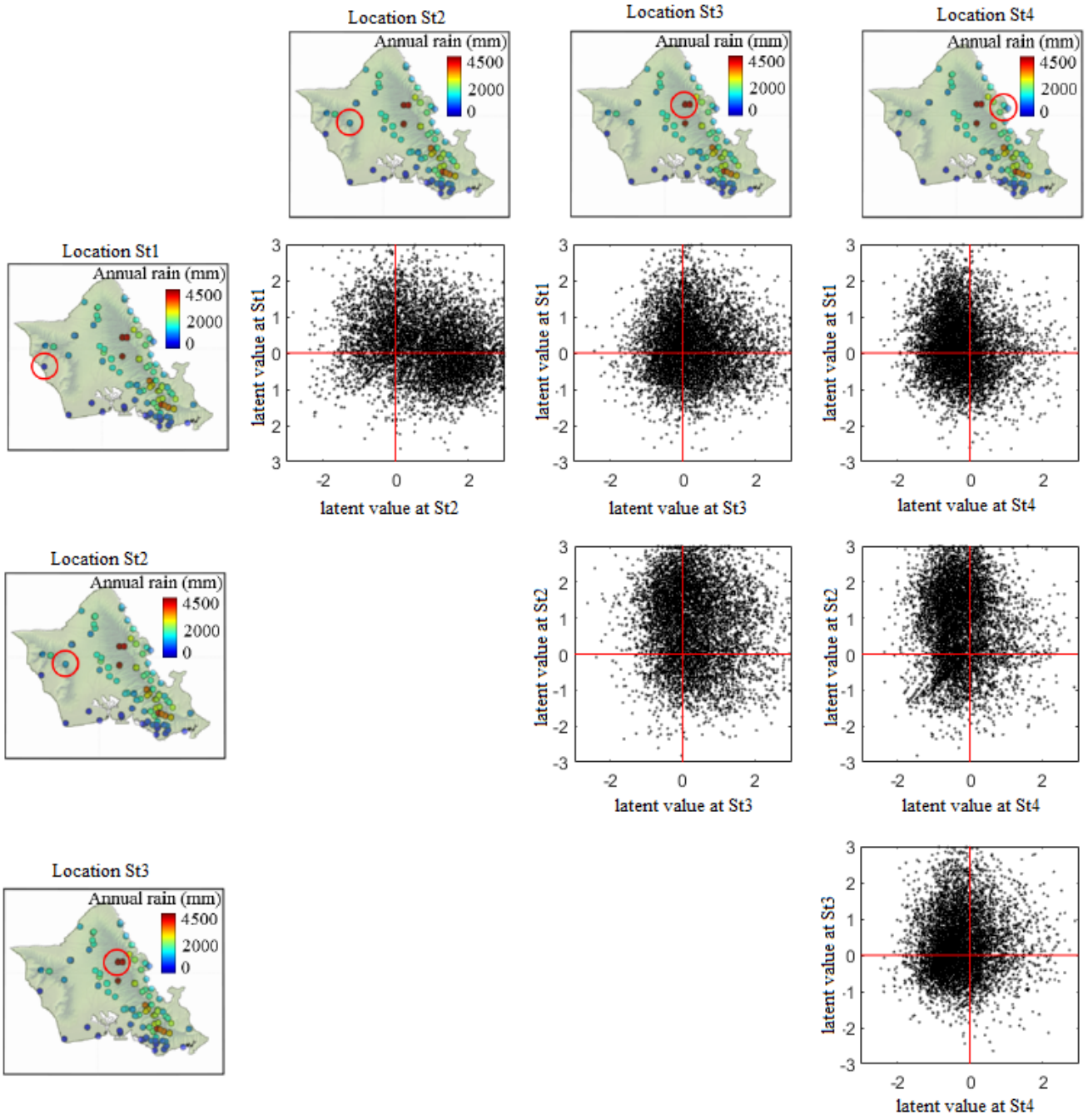

Figure S1: Bivariate scatterplots of latent values in the island of O‘ahu (same target stations as in Fig. 1 of the main paper). One can observe that bivariate spatial dependences are neither bivariate Gaussian (i.e., scatterplots do not have an elliptical shape) nor stationary (i.e., scatterplots are centered on different means, and have different spreads).

2 Supplementary material 2: Relationships between rain types and meteorological covariates in the island of O‘ahu

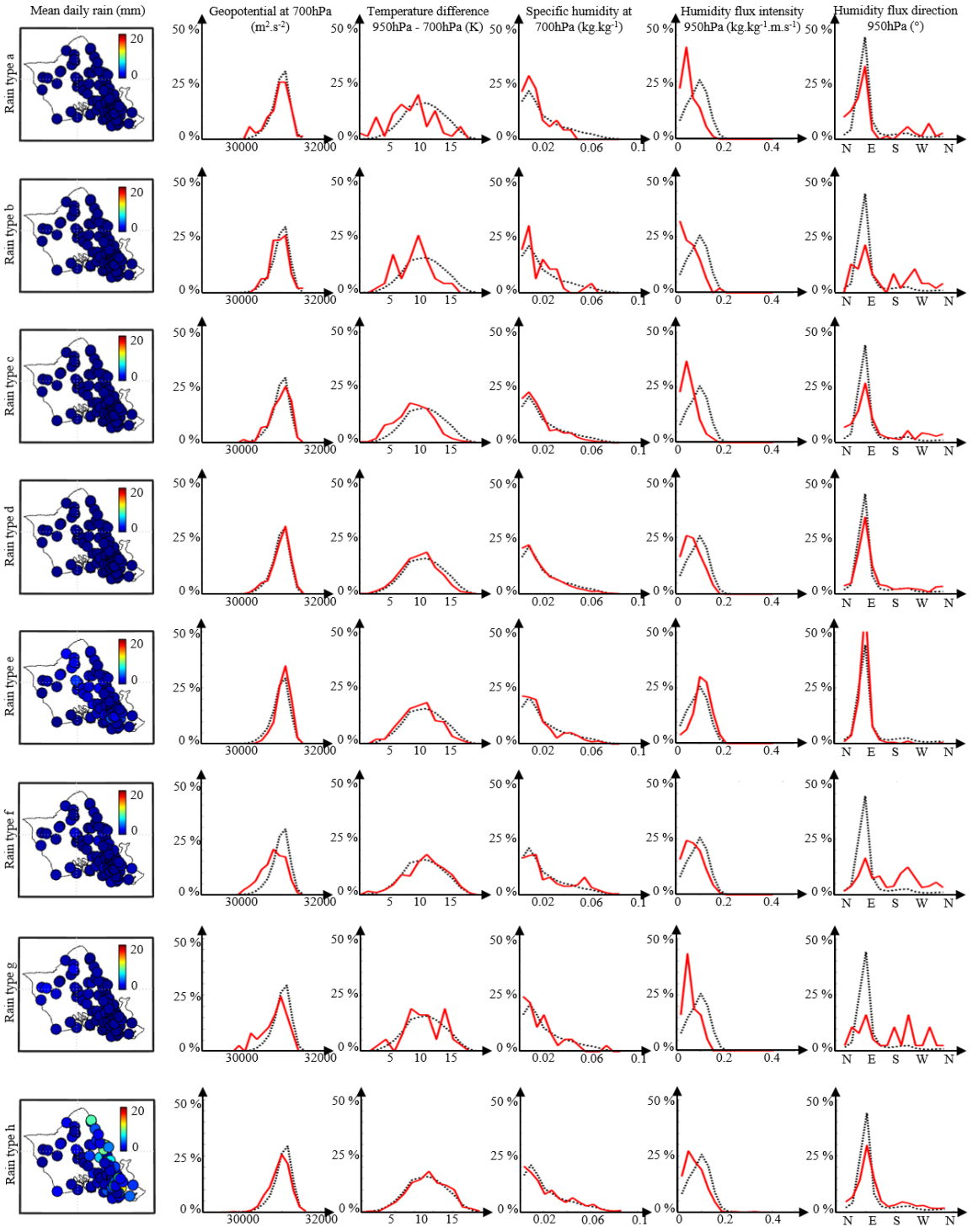

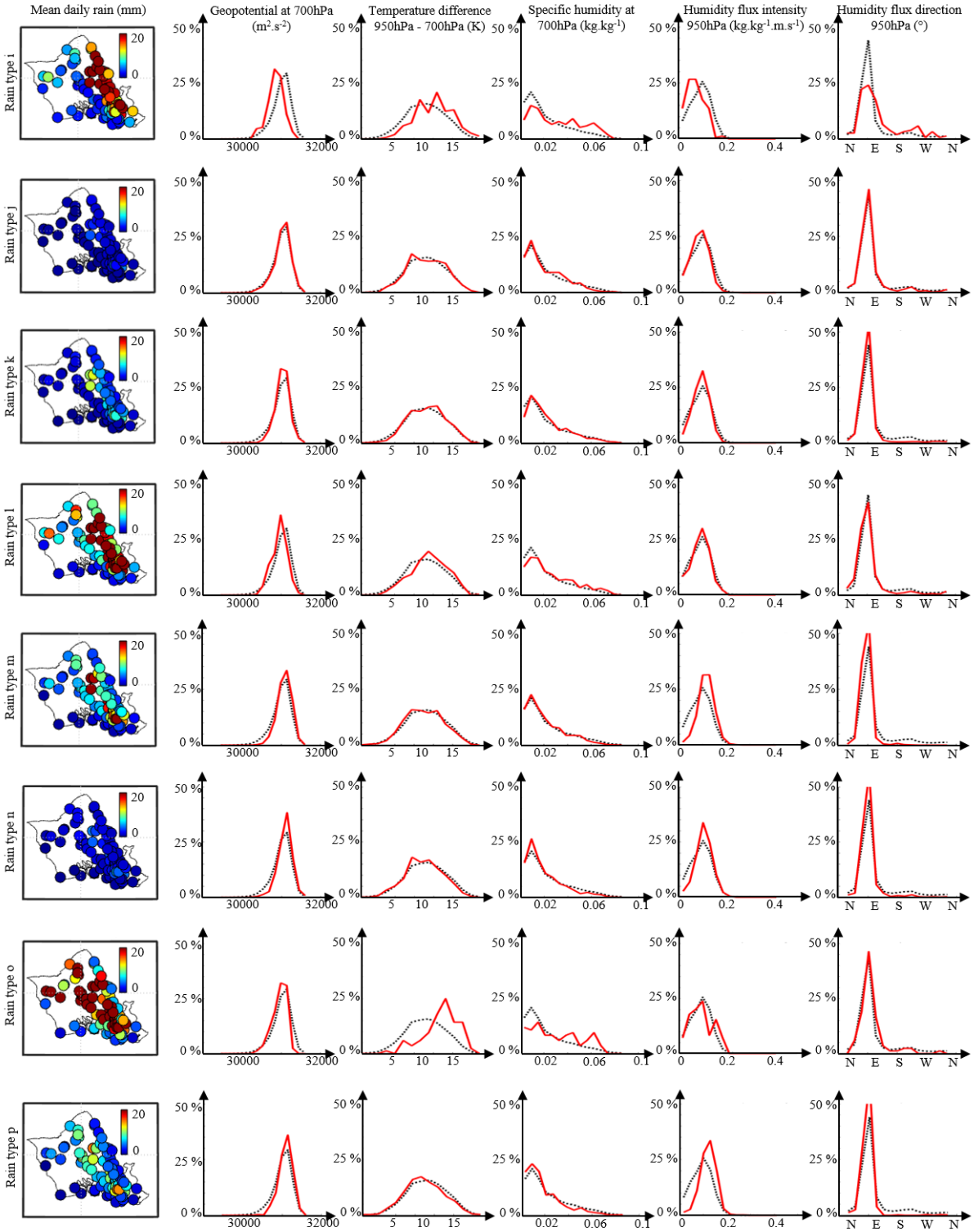
Mean daily rain (mm)
Geopotential at 700hPa (m².s⁻²)
Temperature difference 950hPa - 700hPa (K)
Specific humidity at 700hPa (kg.kg⁻¹)
Humidity flux intensity 950hPa (kg.kg⁻¹.m.s⁻¹)
Humidity flux direction 950hPa (°)
Rain type i
Rain type j
Rain type k
Rain type l
Rain type m
Rain type n
Rain type o
Rain type p
20
0
50 %
25 %
0 %
30000
32000
5
10
15
0.02
0.06
0.1
0
0.2
0.4
N E S W N

19

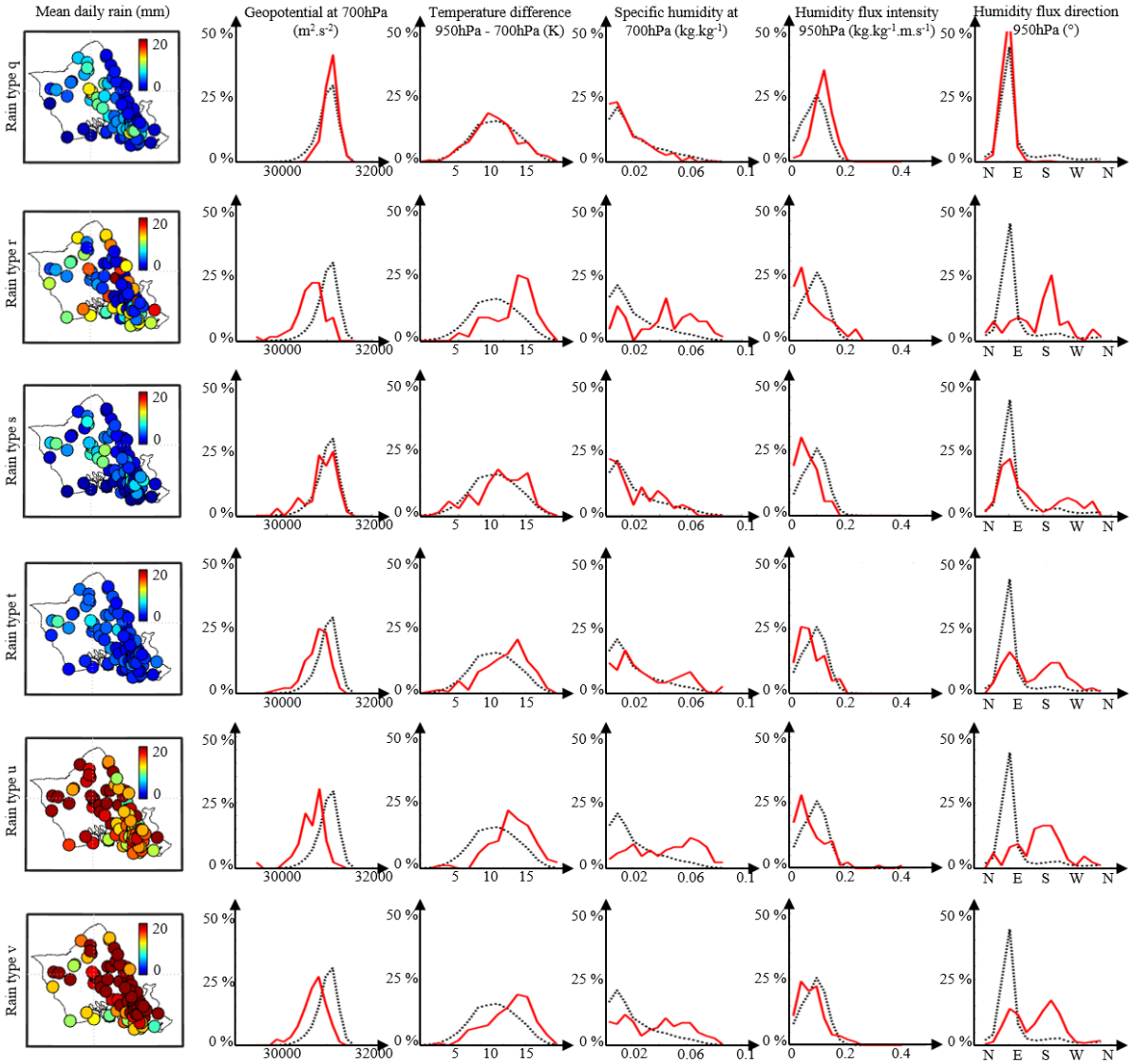

Figure S2: Meteorological covariates observed concurrently with each rain type in the island of O‘ahu. First row: spatial pattern of observed mean daily rain. Second row: geopotential height at 700 hPa. Third row: temperature difference between 950 hPa and 700 hPa. Fourth row: specific humidity at 700 hPa. Fifth and sixth rows: intensity and direction of the specific humidity flux (i.e., wind multiplied by specific humidity) at 950 hPa. In rows 2–6, the red line denotes the pdf for the covariate at hand for the rain type of interest, and the dashed black line denotes the pdf of the same covariate for the entire dataset (i.e., encompassing the 22 rain types).

3 Supplementary material 3: Pdfs of island-scale statistics for the cross-validation of the O‘ahu case study

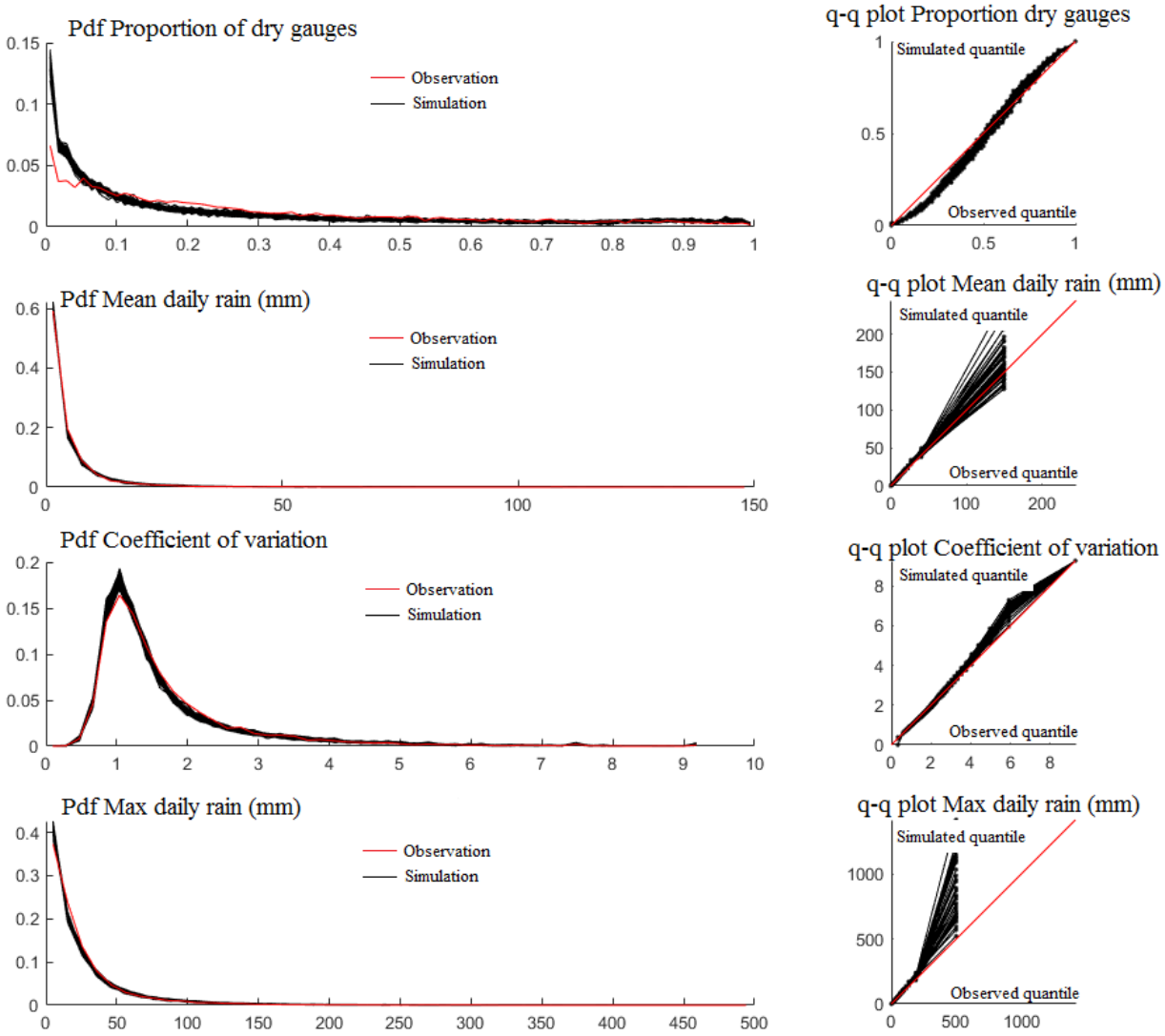

Figure S3: Pdfs of island-scale statistics for the cross-validation of the O‘ahu case study. Observed (red) and simulated (black) probability distribution function (pdf, left) and quantile-quantile plot (q-q plot, right) of the four island-scale rain statistics evaluated in the cross-validation of the main paper (Sect 3.4). From top to bottom: proportion of dry gauges, mean daily rain, coefficient of variation, max daily rain.

4 Supplementary material 4: Model assessment for the island of Tahiti

4.1 Observation dataset and rainfall climatology

The island of Tahiti is located in the South Pacific (lon = 149.5°W, lat = 17.6°S, area = 1042 km^2, max altitude = 2241 m) in French Polynesia. It has been selected to complement the case study of O'ahu because Tahiti experiences a wetter climate (mean annual rain exceeding 10000 mm/year at Mt Mauru, Fig. SM4.1) with a strong rain seasonality caused by the influence of the South Pacific Convergence Zone (SPCZ) [*Laurent et al.*, 2019] [*Brown et al.*, 2020]. The SPCZ crosses Tahiti during (austral) summer (November–April), which leads to a marked wet season (Fig. SM4.3) [*Hopuare et al.*, 2015]. Despite the above differences in rain intensity and seasonality, O'ahu and Tahiti share similar patterns of orographic rain enhancement because both have significant topography and are exposed to a tropical marine climate. Hence, the windward (northeast) and high altitude slopes of Tahiti tend to be wetter than their leeward and lowland counterparts. In terms of rain generation processes, Tahitian precipitation is dominated by orographic rains triggered by easterly trade winds [*Laurent et al.*, 2019], complemented by a significant contribution from regional atmospheric disturbances driven by the Madden-Julian Oscillation (MJO) [*Hopuare et al.*, 2018].

To explore the features of Tahitian rainfalls, we use an 11-year dataset covering the period 2004–2014 and encompassing 26 rain gauges operated by the French weather agency (Météo France) and Direction of Equipment of Tahiti (Groupement d'Etudes et de Gestion du Domaine Public de Polynésie Française [GEGDP]). This dataset has been compiled and quality controlled by [*Pheulpin*, 2016] and occasional gaps were filled for the present study using the non-parametric vector sampling approach [*Oriani et al.*, 2020].

4.2 Rain types in Tahiti

Applying the rain typing approach introduced in Sect. 2.2.3 to the above dataset leads to 11 rain types for the period 2004–2014 (Fig. SM4.1). Scrutinizing the spatial patterns of mean daily rainfall (Fig. SM4.1), seasonality of rain type occurrence (Fig. SM4.1), and relationships with meteorological covariates (Fig. SM4.2) led us to pool rain types into three hyperclasses (H1-3) that can be linked to the three main rain generation processes in the area.

(H1) Almost dry days (Fig. SM4.1, rain types a–c): during these days, most rain gauges report no rain and no gauge reports more than 5 mm/day on average. In terms of weather conditions, these types are associated with a stable atmosphere and low moisture influx (Fig. SM4.2).

(H2) Trade wind days (Fig. SM4.1, rain types d–g): these types display well-defined spatial patterns of rain accumulation caused by orographic lifting and are associated with a relatively stable atmosphere and an important influx of moisture under the influence of east-northeasterly trade winds (Fig. SM4.2).

(H3) Regional atmospheric disturbance days (Fig. SM4.1, rain types h–k): these days correspond to relatively widespread rains with latitudinal gradients; two sub-categories can be identified. The first one encompasses rain types h–j that occur mostly during the wet season (November–April) and are associated with low pressure, unstable atmosphere, weak trade wind inversion, and weak northerly winds (and therefore moisture influx). These types probably correspond to convective rains caused by the interactions between the MJO and the crossing of the SPCZ over Tahiti. The second category encompasses a single type (type k) and is associated with southeasterly winds. This type probably corresponds to "Maraamu" events (Tahitian name [Laurent et al., 2019]), i.e., days with unusual southeasterly trade winds. This type has been placed in the disturbance hyperclass (H3) category because it is relatively rare, but, with the exception of wind direction, the associated meteorological covariates are close to those of trade wind days (Fig. SM4.2).

The pooling of rain types in three hyperclasses with names similar to the ones used for the O'ahu case study should not hide the differences in rain generation processes between the two islands. Hence, while orographic rain enhancement by orographic lifting probably follows relatively similar processes in both islands (although modulated by differences in island morphology), disturbance related precipitations are produced by very different processes: mid-latitude or sub-tropical weather systems in the case of O'ahu; and purely tropical effects caused by the transit of the SPCZ in the case of Tahiti.

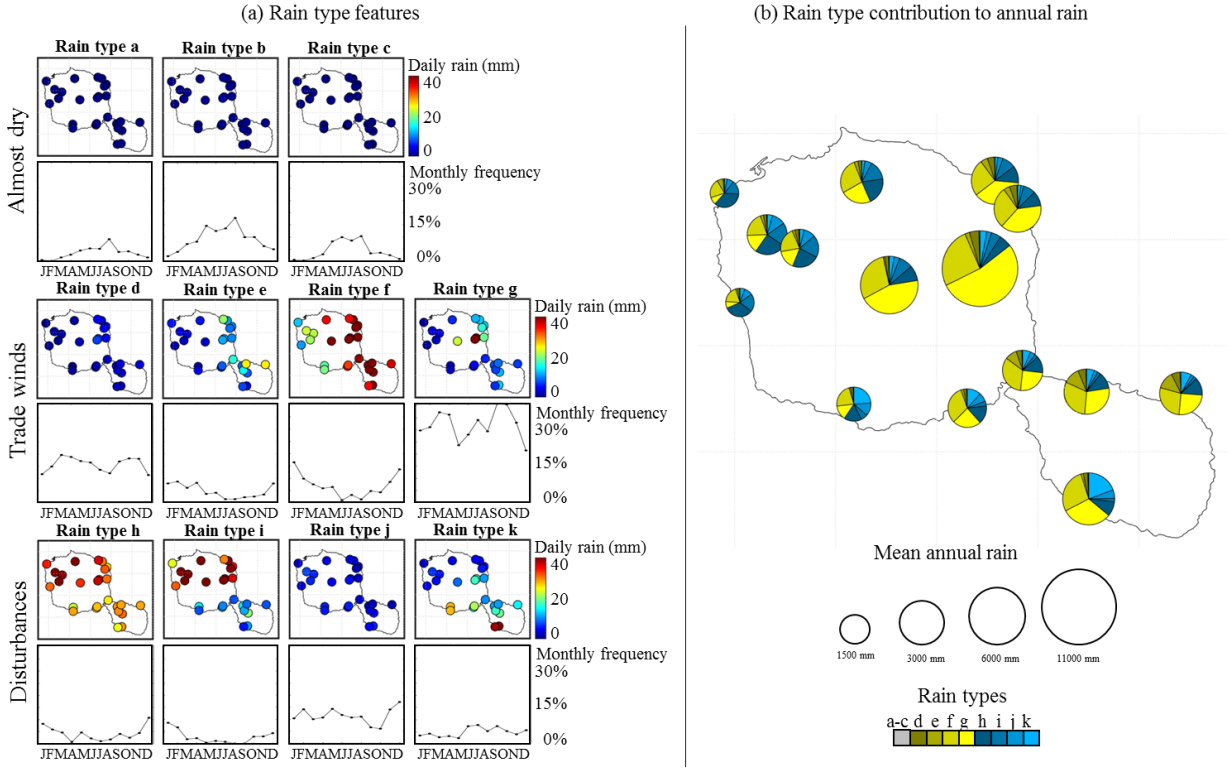

Figure S4: Rain types identified for the island of Tahiti. (a) Spatial distribution and frequency of occurrence of each rain type. (b) Contribution of each rain type to the annual rain accumulation for a selection of 15 gauges spread throughout the island.

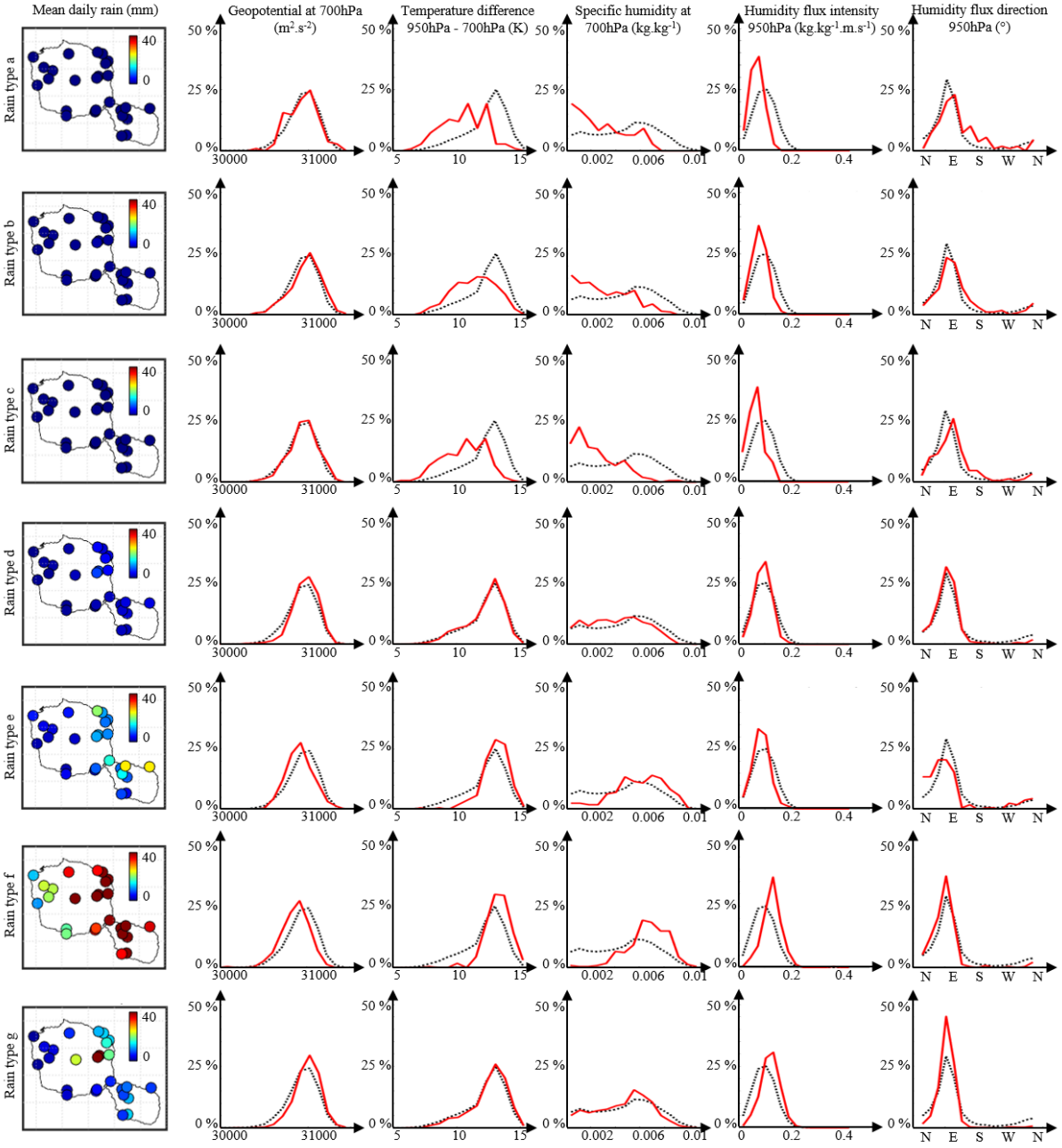
Mean daily rain (mm)
Geopotential at 700hPa (m².s⁻²)
Temperature difference 950hPa - 700hPa (K)
Specific humidity at 700hPa (kg.kg⁻¹)
Humidity flux intensity 950hPa (kg.kg⁻¹.m.s⁻¹)
Humidity flux direction 950hPa (°)
Rain type a
Rain type b
Rain type c
Rain type d
Rain type e
Rain type f
Rain type g
40
0
50 %
25 %
0 %
30000
31000
5
10
15
0.002
0.006
0.01
0
0.2
0.4
N
E
S
W
N

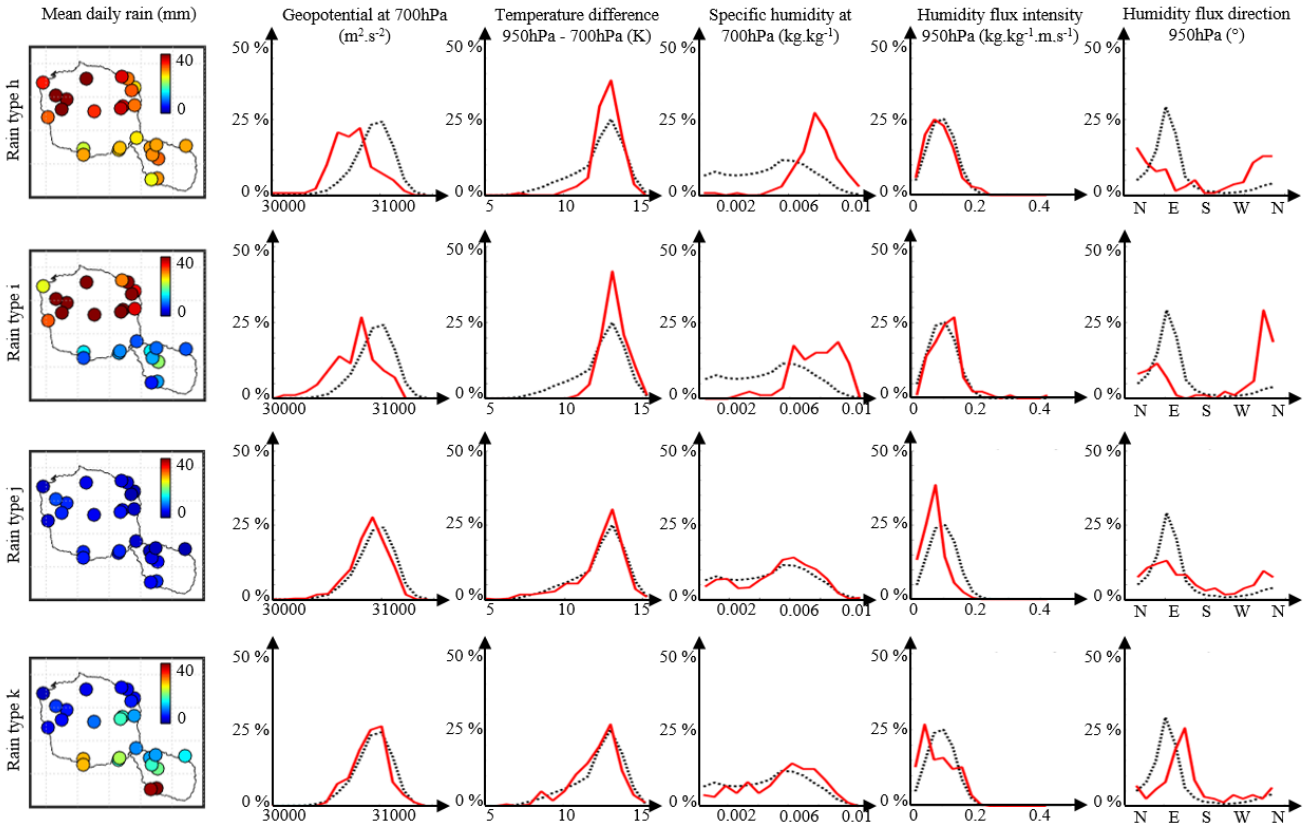

Figure S5: Meteorological covariates observed concurrently with each rain type for the island of Tahiti. First row: spatial pattern of observed mean daily rain. Second row: geopotential height at 700 hPa. Third row: temperature difference between 950 and 700 hPa. Fourth row: specific humidity at 700 hPa. Fifth and sixth rows: intensity and direction of the specific humidity flux (i.e., wind multiplied by specific humidity) at 950 hPa. In rows 2–6, the red line denotes the pdf for the covariate at hand for the rain type of interest, and the dashed black line denotes the pdf of the same covariate for the entire dataset (i.e., encompassing the 11 rain types).

4.3 Model cross-validation for the island of Tahiti

Figures SM4.3 and SM4.4 evaluate the ability of the proposed stochastic rainfall model to simulate site-specific and island-scale statistics, respectively, for the island of Tahiti. Results show that the model performs very well for this island. In particular, note the ability of the model to faithfully reproduce rainfall seasonality, which is a distinctive feature of Tahitian rainfalls when compared to the O'ahu case study presented in the main text. In addition, contrary to the O'ahu experiment, the island-scale 11-year extreme precipitation is accurately simulated in the case of Tahiti.

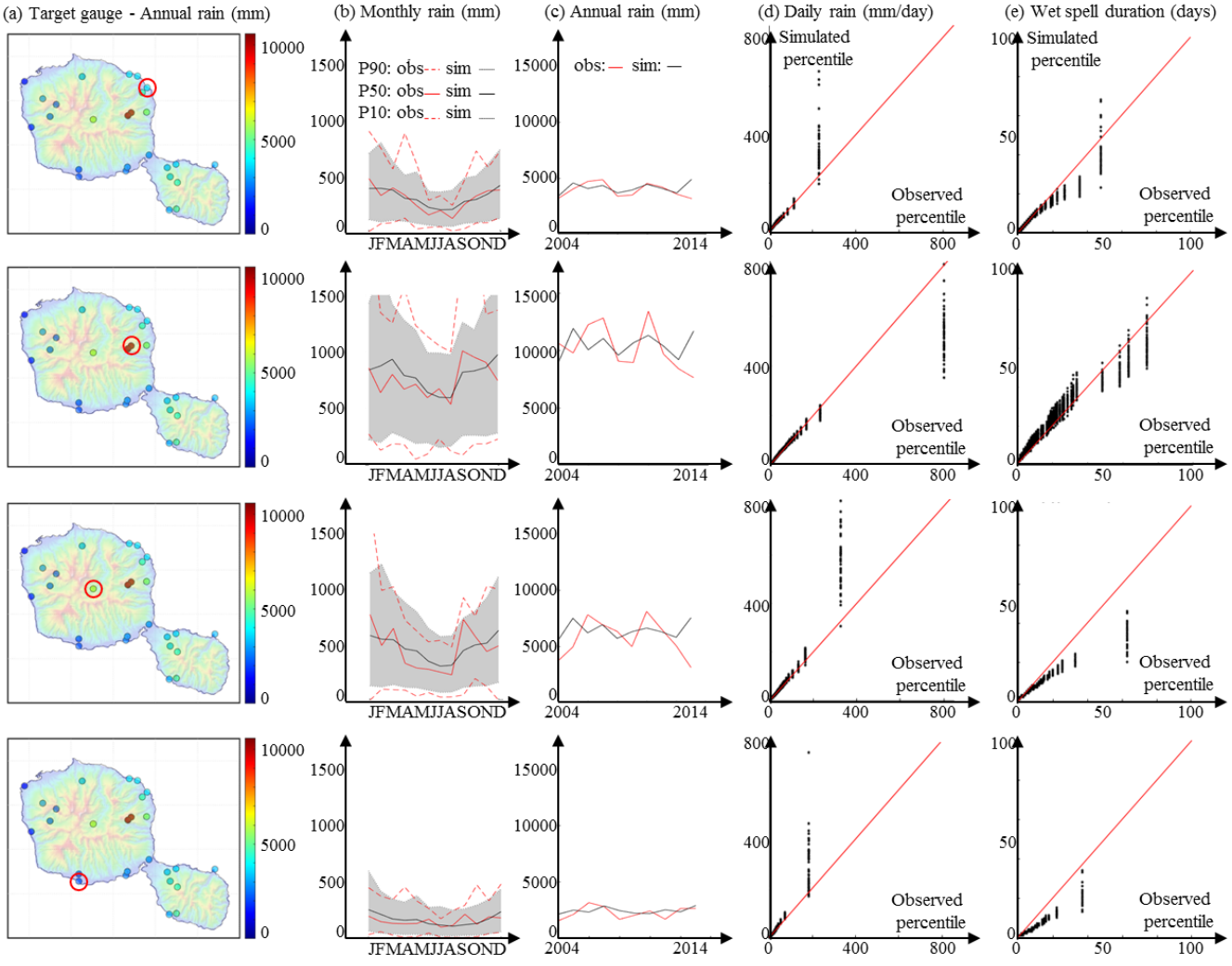

Figure S6: Ability of the model to simulate site-specific rain statistics on Tahiti. (a) Target locations. (b) Observed (red) and simulated (black) monthly rain accumulation. Dashed lines denote quantiles 10% and 90%, and solid lines denote the quantile 50%. In the case of simulations (black), for readability, we report in the figure only the median of each quantile (10%, 50%, 90%) instead of 50 simulated quantiles. (c) Observed (red) and simulated (black) annual rain accumulation. In the case of simulations (black), for readability, we report in the figure only the median of the 50 simulations. (d) The q-q plot of daily rain percentiles. (e) The q-q plot of wet spell duration percentiles.

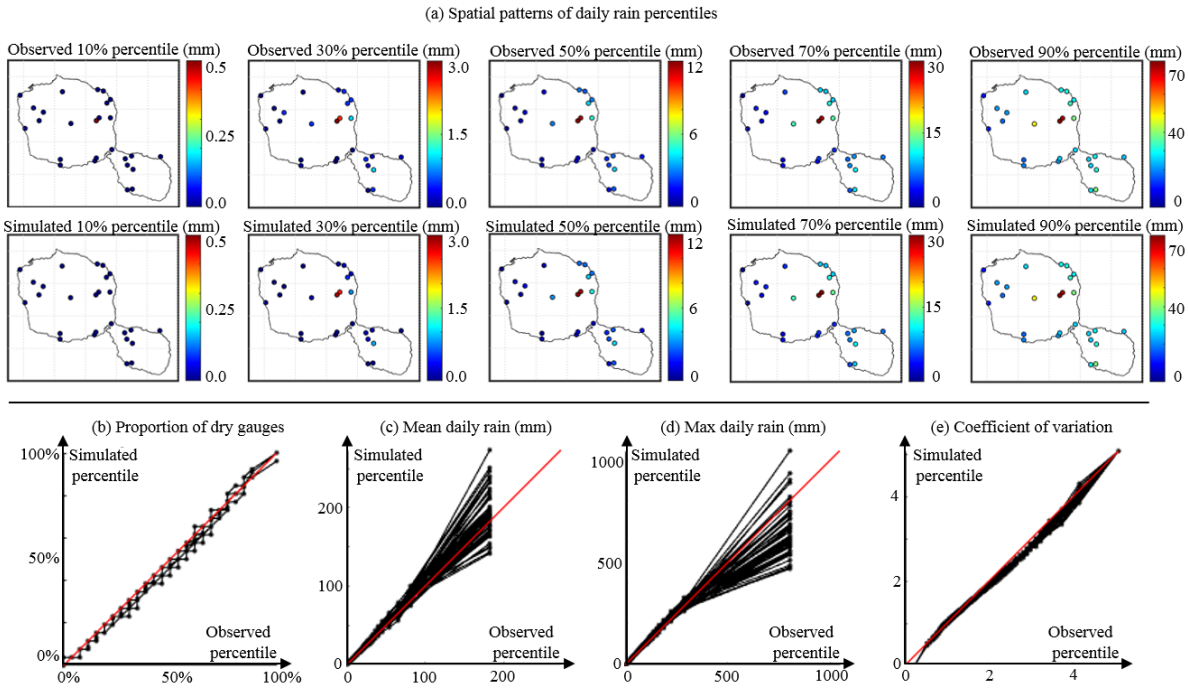

Figure S7: Assessment of island-scale statistics simulation in Tahiti. (a) Spatial patterns of observed (upper row) and simulated (lower row) percentiles of daily rain accumulation. From left to right: 10%, 30%, 50%, 70% and 90% percentiles. (b–d) The q-q plots of key rain statistics aggregated over the whole rain gauge network: (b) proportion of dry gauges; (c–d) mean and max daily rain; (e) coefficient of variation.

References

Brown, J. R., Lengaigne, M., Lintner, B. R., Widlandsky, M. J., van der Wiel, K., Dutheil, C., Linsley, B. K., Matthew, A. J. and Renwick, J.: South Pacific Convergence Zone dynamics, variability and impacts in a changing climate, Nature Reviews Earth and Environment 1, 530-543, https://doi.org/10.1038/s43017-020-0078-2, 2020.

Hopuare, M., Pontaud, M., Céron, J.-P., Ortega, P., and Laurent, V.: Climate change, Pacific climate drivers and observed precipitation variability in Tahiti, French Polynesia, Climate Research, 63, 157-170, https://doi.org/10.3354/cr01288, 2015.

Hopuare, M., Guglielmino, M. and Ortega, P.: Interactions between intraseasonal and diurnal variability of precipitation in the South Central Pacific: The case of a small high island, Tahiti, French Polynesia, International Journal of Climatology, 39, 670-686, https://doi.org/10.1002/joc.5834, 2018.

Laurent, V., Maamaatuaiahutapu, K., Brodien, I., Lombardo, S., Tardy, M., and Varney, P.: Atlas climatologique de la Polynésie française, 232 pp., Météo France, Délégation interrégionale de Polynésie française, 2019.

Oriani, F., Stisen, S., Demirel, M. C., and Mariethoz, G.: Missing data imputation for multisite rainfall networks: A comparison between geostatistical interpolation and pattern-based estimation on different terrain types, Journal of Hydrometeorology, 21, 2325-2341, https://doi.org/10.1175/JHM-D-19-0220.1, 2020.

Pheulpin, L. : Fonctionnement hydro-sédimentaire d'un petit bassin versant en climat tropical humide : La Titaaviri, île de Tahiti, Polynésie française, 230 pp, Université de la Polynésie Française, Papeete, French Polynesia, 2016.